JMEPEG (2008) 17:302–315
DOI: 10.1007/s11665-008-9230-8

©ASM International
1059-9495/$19.00

Investigation of Liquid Impact-Based Macro-, Meso-, and Microforming Processes

V. Samardzic, E. S. Geskin, G.A. Atanov, A.N. Semko, and A. Kovaliov

(Submitted October 18, 2007; in revised form March 6, 2008)

It was shown that the liquid impact at the projectile speed of 1500 m/s affects a target similarly to an explosive deposited on the workpiece surface. A setup to investigate material deformation using the liquid impact was designed and constructed. The setup entailed a launcher for the acceleration of projectiles, a female die, a device for measuring the projectile momentum at the impact zone and a fixture for fastening the launcher and the die. The experiments included punching, stamping, extrusion, and forging, Special attention has been paid to the study of the microscale forging and extrusion. Forming of steel, spring steel, brass, aluminum, and copper samples was investigated. Dimensional stability and surface topography of the samples generated in the course of performed experiments were examined. The feasibility and effectiveness of the application of liquid impact for metal forming were shown.

Keywords extrusion, liquid impact, liquid projectile, macro, meso, microchannel, microforming, punching, stamping

1. Introduction

The objective of the performed study was to investigate the application of high-speed liquid projectiles for material forming, specifically for formation of macro, submillimeter, and micron scale parts. The processes included punching, forging, extrusion, stamping, submillimeter forging, microscale forging, and extrusion. The technology in question involves impacting a workpiece supported by a die by a high-speed (1000-1750 m/s) water projectile (an impulsive jet) (Ref 1-5). The projectiles are generated by a launcher (a water cannon), which constitutes a modified gun, loaded by a round where a solid slug is replaced by a container with a liquid, e.g. water (Fig. 1). The powder explosion accelerates water and at the end of the barrel the water speed is comparable with that of a solid projectile. The further acceleration occurs in a nozzle attached to the barrel. This enables significant increase of the water velocity. In the previous experiments, a water velocity of 1750 m/s was achieved. Computations show that it is possible to achieve water speed as high as 3-4 km/s. At the speed of 1500 m/s, the pressure exerted on a target at the impact zone is in an order of 1 GPa. At such a pressure a metal target impacted by a liquid projectile acquires the shape of a supporting die. Thus the liquid impact can be used for metal forming and the high-speed liquid projectile can replace a punch.

A water projectile impacting a solid surface at the speed of 1000 m/s and more acts as an explosive, which detonates on the target's surface. Advantages of the impact-based forming (Ref 6) as well as the explosive forming (Ref 7, 8) are well understood and documented. In a number of applications, however, the use of an explosive is difficult if not impossible. In this case high-speed liquid projectiles can be used as a forming tool (Ref 9). Previous research showed the feasibility of the application of the liquid impact to the microforming (Ref 10). In fact, the most promising application of the liquid projectile is mass production of Micro Electro Mechanical Systems parts.

Meso- and microforming is fabrication of parts or structures with at least two dimensions in the submillimeter range by the use of a forming technology. Specifically, in this study mesoforming was defined as the intermediate range between macro- and microscales which is the submillimeter range between 1 mm and 0.1 mm. Microforming was defined as a fabrication of parts or structures with at least two dimensions below 200 μm range. The effectiveness of the application of the plastic deformation for mass production of parts of a wide-dimensional range is quite obvious. It could be the only practical way for mass production of metal and alloy microparts. On the microscale, the use of a liquid impact for punching, extrusion, and forging can be competitive to the existing forming technologies. While implementation of the microfabrication will revolutionize the MEMS fabrication technology, substantial obstacles are to be overcome to achieve this goal. The microforming cannot be developed just by scaling down existing forming processes. New techniques must be found for microscale deformation of various technological materials at a desired rate and accuracy and at an acceptable cost. While in previously conducted study (Ref 10) the demonstrated feasibility of use of liquid projectile impact for microforming, in this study deeper investigation of the accuracy of generated features and effect of the liquid impact on mechanical properties of an impacted material is the objective.

This article was presented at Materials Science & Technology 2007, Automotive and Ground Vehicles symposium held September 16-20, 2007, in Detroit, MI.

V. Samardzic and **E. S. Geskin**, New Jersey Institute of Technology, 292 Lawton Avenue #44, Cliffside Park, NJ 07010; and **G.A. Atanov, A.N. Semko,** and **A. Kovaliov**, Donetsk National University, Donetsk, Ukraine. Contact e-mail: vxs9076@njit.edu.

Deformation of a target material in the course of a high-speed liquid impact was investigated experimentally. The performed study involved punching, extrusion and forging of various metals including micro- and submillimeter stamping and extrusion. The performed experiments showed that high-speed liquid projectiles have a potential of becoming a competitive forming tool. Of course a number of issues pertinent to the selection of the energy source for the water acceleration, energy transfer from a source to the projectile, reliability of the launcher and a guiding system, die design and reliability, etc. must be addressed. However, the feasibility to generate a desired deformation of a target material, regardless of scale, using the liquid impact was demonstrated by the performed experiments and analysis.

2. Existing Forming Technologies

Impact forming is a traditional manufacturing technology (Ref 6). A hammer is a common forming tool. It was found, however, that the process effectiveness improves as the rate of the energy transfer in the course of the impact increases. Currently, the impact based high energy rate forming (HERF) processes such as the explosive forming, magnetic-pulse forming, and electrohydraulic forming are widely used for materials shaping (Ref 7, 8) as well as for the improvement of materials properties, welding, sintering, composites fabrication, etc. (Ref 8). In HERF processes, the punch is replaced by a compression waves emanating from the explosion site. Thus, only one die is needed. However, the existing HERF processes can be improved still further. Research in micro- and meso-manufacturing areas is being conducted by a team lead by Dohda (Ref 11), Gifu University, Japan. Micropressing technology has been developed. This technology involved formation of the ultra fine holes in aluminum samples using 15 μm SiC fibers as a punch. Microforging was used to die forge microparts out of amorphous alloy. Microextrusion of aluminum alloys was investigated as well. A single process system was designed and used for each application (micropress, microextruder). Development of a system which could be used for more than a single microforming application and which would have higher efficiency was addressed by a group of Hye-Jin Lee of Korean Institute of Industrial Technology, Korea (Ref 12). Study of forming of the submillimeter metal parts is currently being carried out in the Friedrich-Alexander University, Germany (Ref 13). A Group Mass-micro of Dr. Jiangho Lin, University of Birmingham, UK), is currently working on the development of technologies of mass production of microparts (Ref 14). While the teams above are involved in one or another miniaturization of forming facilities, the objective of the proposed study is modification of the mode of the generation of the stress field in a target.

3. Experimental Technique

An experimental setup (Fig. 2), for the study of the liquid impact-based forming was designed and constructed. In this setup samples to be processed were mounted on a heavy

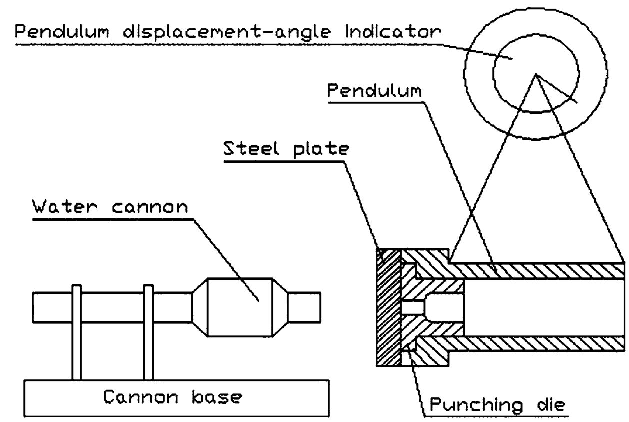

Fig. 2 Schematic of the experimental setup. Notice that mounting of the target on a ballistic pendulum allows measuring the impact momentum

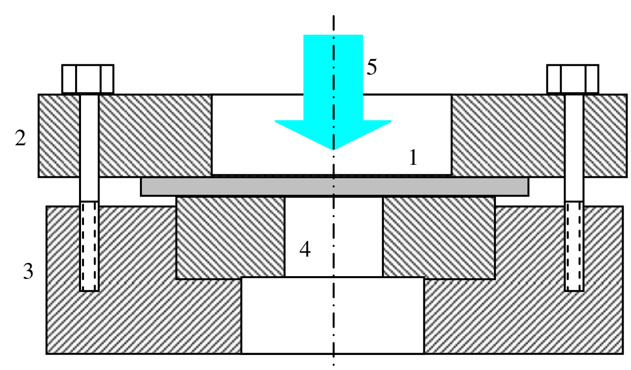

Fig. 3 Sample—1, clamping plate—2, die holder—3, die—4, and high-speed liquid projectile—5

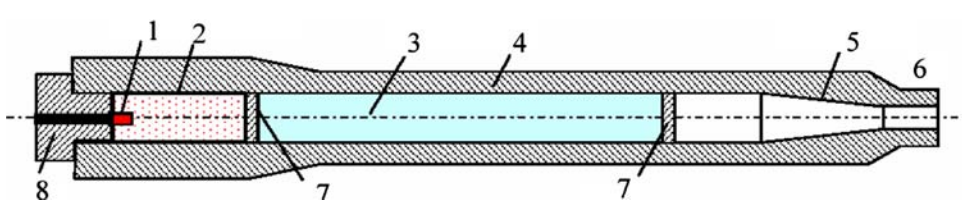

Fig. 1 Water launcher schematic: 1—primer, 2—combustion chamber, 3—water, 4—barrel, 5—nozzle, 6—collimator, 7—nonporous membrane, and 8—initiating subassembly

pendulum which was displaced by the water impact. The angular displacement of pendulum was measured in each experiment and the projectile impulse and momentum were calculated by the use of the measured pendulum displacement. During an experiment, the water cannon (Fig. 1) was placed at a desired distance from a sample which then was impacted at selected conditions. In the course of the impact, the target acquired a shape of a supporting die. The principal challenge in the die fabrication was formation of submillimeter and micron scale cavities using conventional machining facilities (lathe, milling machine, etc.). During each experiment, the values of water mass, powder mass, standoff distance, and pendulum displacement were measured and the acquired data were incorporated into a global matrix of the investigation. Upon completion of an experiment generated samples were examined visually and then sample characterization, involving scanning electron microscopy, infinite focus microscopy, optical microscopy, 3D digital microscopy, and 3D digital profiler, was carried out.

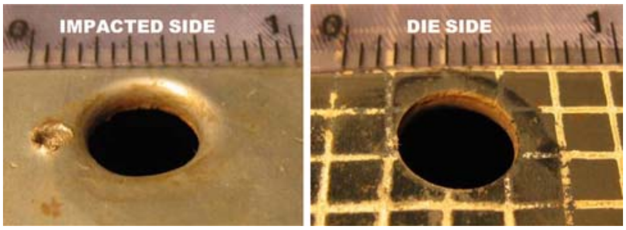

Fig. 4 Piercing of a spring steel. Notice feasibility of precision deformation of a difficult-to-shape material, $h = 3.175$ mm, $D = 10$ mm

Table 1 Punching of steel experimental results

Experiment number	Plate thickness, mm	Die diameter, mm	Result	Calculated projectile velocity, m/s
1	4	16.5	Punched	1500
2	6	16.5	Punched	1500
3	8	16.5	Punched	1500
4	10	16.5	Not punched	1500
5	4	25	Punched	1500
6	8	25	Punched	1500
7	10	25	Punched	1500

The fabricated dies enabled us to examine various micro-forming technologies. Both, the submillimeter and micron scale deformations were investigated. The study involved filling cavities by a target material and stamping a die shape on the target surface. The filling of the semi-closed cavities (groves on the workpiece surface) and metal extrusion into open micron scale slots was examined. Stamping using simple (cylindrical wires) and complex (a coin) dies was also investigated. Targets were fabricated from copper, brass, aluminum, and steel. In one of the performed experiments, extrusion of an alloy used for fabrication of Ukrainian coins was studied.

In the course of the performed experiments, water was propelled by the products of the combustion of a gunpowder. The standoff distance was 16 cm in all experiments. Calculated outflow velocity of the projectile head ranged between 850 and

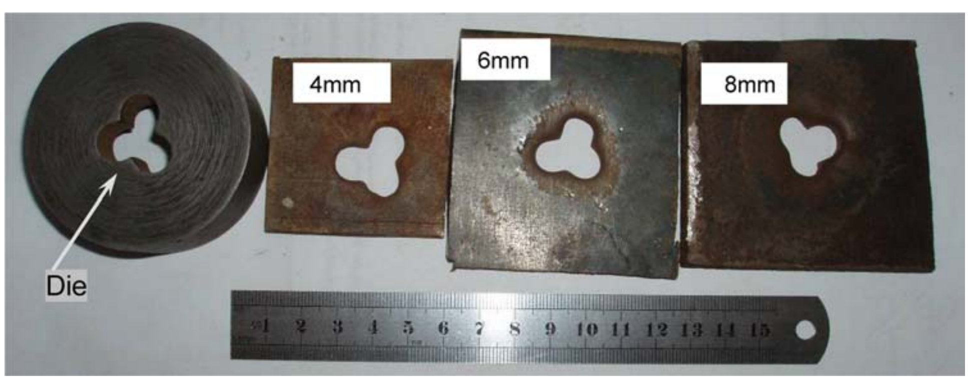

Fig. 5 Formation of shaped openings using a round jet. Notice that the workpiece thickness does not affect the accuracy of the piercing

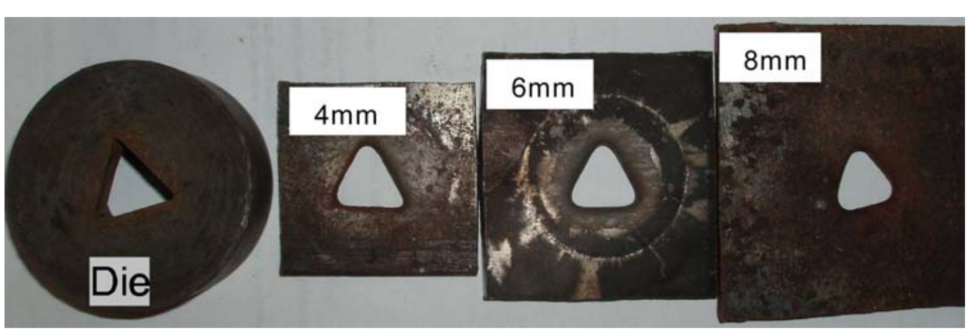

Fig. 6 Formation of triangular openings using a round jet. Notice that the workpiece thickness does not affect the accuracy of the piercing

1566 m/s. Calculated maximal pressure inside the nozzle ranged from 341 and 843 MPa. At these conditions, the pressure excerted on the workpiece varied from 0.35 to 1.2 Gpa.

4. Experimental Investigation of Punching Steel Plates

4.1 Punching Circular Openings

Three objectives were pursued in this study. First, the feasibility and limits (maximal plate thickness, minimal, and maximal punched opening diameters) of the operation were explored. Second, punching of complex shape opening in steel plates of various thicknesses was studied. The third objective was to investigate punching of multiple holes by the impact a single water projectile. A close-up schematic of the impact zone subassembly is shown in Fig. 3. Dies for punching steel plates were designed and manufactured out of a die-steel and then were heat treated.

Fig. 7 Formation of the multiple openings by a single impact of a round jet. Steel sheet thickness is 2.5 mm and the opening diameter is 4 mm. Notice that the liquid penetration into the workpiece can be controlled by the impact condition

Hot-rolled carbon steel with 0.22% of the carbon content which has the tensile strength of 450 MPa, the yield strength of 320 MPa, and the maximal relative elongation (plasticity) of 26% was used for the samples fabrication in the first series of the experiments. Plates having 2.5, 4.2, 6, 8, and 10 mm thicknesses were tested. In each experiment, a steel sample was tightly attached against the die and mounted on a pendulum. Dies with round openings of 16.5 and 25 mm diameter were used in this part of investigation. Against both dies circular openings were created in plates of 2, 4, 6, and 8 mm (Ref 9). The opening of 25 mm diameter was created in the 10-mm thick plate while the opening of 16.5 mm diameter was not completed in the similar plate. In this case the deformation process on the impact side has been initiated and shearing cutting on the die side was started, but not completed. Entering side of each opening (Fig. 4) has slightly rounded edges due to the flow of the punched portion of material and exiting side of circular opening has sharp edge which was cut against the die. Calculated velocity of the projectile head prior to the impact was 1500 m/s.

Another series of experiments involved evaluation of the maximal opening generated by the impacting jet. In these experiments, the 4-mm thick steel plates were punched against dies with the openings of 4, 8, 10.5, 16.5, 20.5, 25, 35, 40, and 45 mm. An array of clean-cut openings was created against dies with: 4, 8, 10.5, 16.5, 20.5, 25, 30, and 35 mm diametric openings. The attempt to generate the opening of 40 mm failed. The sample was pierced and it failed in petaling mode. Diametric opening of 45 mm was punched around ¾ of the circumference and a punched portion of the material was still holding on ¼ of the circumference. In this part of the investigation, $D/d = 2.5$ was reached and the maximal thickness of $h = 0.67d$ was punched. Here D is the opening diameter, mm; d is the projectile diameter, mm, and h is the standoff distance. Selected experimental results are shown in Table 1.

The samples generated in each experiment were visually examined and material flow indicators were identified. For example in the experiment 4 metal was deformed, sheering started, but opening was not punched. In the experiment 7a, high-quality opening was punched. An exiting side of the opening had a sharp edge with a diameter equal to the diameter

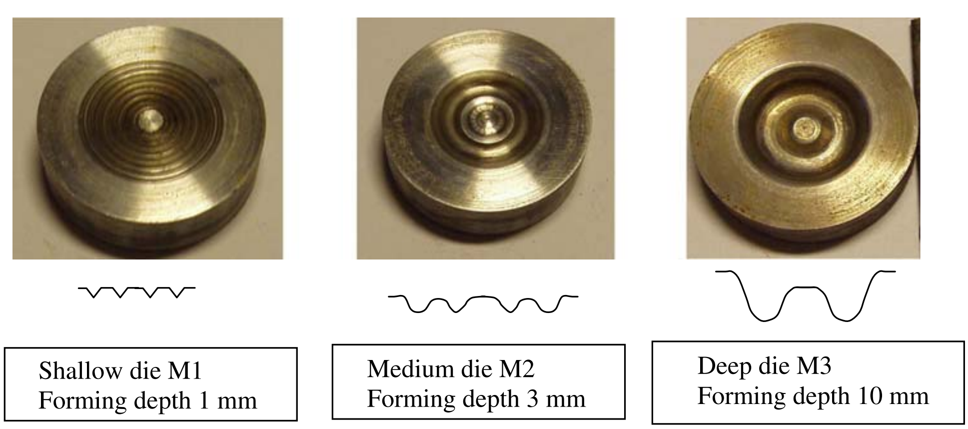

Fig. 8 Forming dies

of the die opening while impact side has slightly smaller diameter with rounded edges.

Investigation of punching of high-elasticity spring steel was carried out as well. Spring steel 3.175 mm thick was punched against a die with a circular opening 10 mm in diameter (Fig. 4). In the performed experiments, an array of various round openings was created at a single (15 mm) projectile diameter. This shows that a high-speed water projectile is an effective punching tool. Thus, a novel material processing operation has been demonstrated.

4.2 Punching of Complex Shape Openings

In these experiments, steel plates of various thicknesses were punched against dies of three different shapes. In the first series of experiments, a die contained three overlapping circulars having the same diameter of 15 mm. The second die had the triangular equilateral opening with 20 mm side. In the third experiment, a die with multiple 4 mm diameter holes placed at 4 mm distance from each other, was used. Experiments with composite circle and triangular openings were performed with steel plates having the thickness of 4, 6, 8, and 10 mm. Repeatability of the results was demonstrated on the various samples.

The performed experiments (Figs. 5-7) show that complex shape openings other than circular can be reproduced by the impact of the circular projectile. Feasibility of new technology introduced in previous part of this work was broadened by this study.

Fig. 9 Results of forming of a 2.5-mm thick, ductile steel sample against a shallow die M1. Die side (*left*), die (*middle*), and impact side (*right*) views

5. Experimental Study of Forging Using High-Speed Water Projectiles

The objective of this study was to demonstrate the potential applications of liquid projectiles to the metal forging. The experiments involved the use of three dies having various geometries. Material of targets used for this part of the investigation included copper, an aluminum alloy, and a high-ductility steel. The steel sample has elongation 46%, tensile strength of 323 MPa, and yield strength of 195 Mpa. It was a high-ductility steel alloy with addition of aluminum generally used for deep drawing, e.g. for forming of housing compressors for refrigerators. The thickness of the steel plates used as targets was 2.5 mm.

Forging was performed against three types of dies: shallow, medium, and deep (Fig. 8). Results of forging are shown in Figs. 9-11 and summarized in Table 2. The obtained results show that the impact pressure is inversely proportional to the distance of the impact center. While at the center of the target the geometry of generated grooves accurately reproduces the geometry of the die, as the distance from the center of the impact increases the compliance between the die and the workpiece reduces and reproducibility of the die image weakens. This experiment demonstrates that there is a zone in the vicinity of impact where precise reproduction of the shape of a die is possible.

In this study, consistency of forming operations was confirmed by repetition of experiments. The stable output was obtained at each test. This experiment showed that forming of deep and complex 3D parts can be accomplished by the high-speed liquid impact. Thus, the proposed material processing technique was validated.

6. Experimental Investigation of Mesoforming

6.1 Formation of Submillimeter Scale Grooves

In our previously study (Ref 10), the feasibility for liquid impact-based submillimeter range was demonstrated and accuracy of forming was demonstrated. The experiments involved the study of formation of submillimeter circumferential ridges on the target surface. For this study, a die with concentric groves was designed and manufactured. The general view of the die surface is depicted in Fig. 12. The design parameters of the die groves are given in Table 3 and Fig. 13 which show a

Fig. 10 Results of forming of a 2.5-mm thick ductile steel sample against a medium die M2. Die side (*left*), and impact side (*right*) views

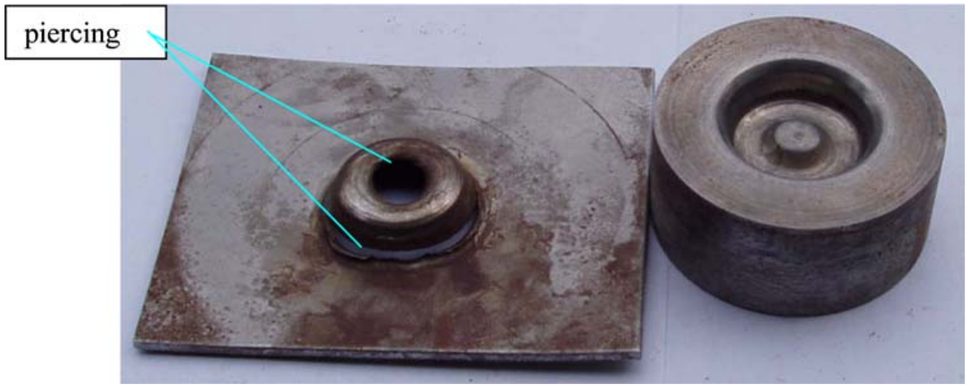

Fig. 11 Results of forming of a 2.5-mm thick ductile steel sample against a deep die M3. Notice the compliance of geometries of the die and the generated part

Table 2 Forming of steel experimental results

Experiment number	Plate thickness, mm	Die	Result	Experimental conditions
1	2.5	M1	Excellent forming	Shallow die M1. High-ductility steel. Die geometry: concentric channels 1 mm deep with step of 2 mm and inclination angle of 90°
2	2.5	M2	Excellent forming	Medium die M2. Cannon shooting mode. High-ductility steel
3	2.5	M3	Sample pierced and cracked	Deep die M3. High-ductility steel. Calculated maximal velocity 700 m/s. Sample pierced and cracked
4	4	M3	Central portion pierced	Deep die (M3). Carbon steel 20
5	6	M3	Central portion pierced	Deep forming (M3). Carbon steel 1020 plate 6 mm thick. Profile almost fully formed
6	6	M3	Central portion pierced	Deep forming (M3). Carbon steel 1020 plate 6 mm thick. Calculated projectile velocity 1500 m/s. Profile fully formed and central portion pierced

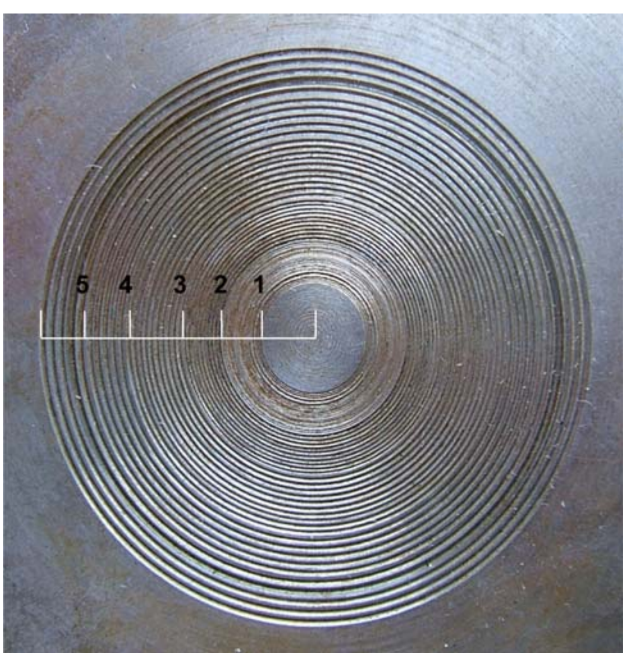

Fig. 12 General view of a die used for fine forging. Notice complexity of the die geometry. Numbers 1-5 are numbers of the section on the die surface

Table 3 Designed parameters of the grooves generated on the die surface

Section	1	2	3	4	5
Step, *h* mm	0.1	0.2	0.3	0.4	0.5
Depth, *b* mm	0.05	0.1	0.15	0.2	0.25
Number of grooves	20	10	10	5	5

Notice difference in groove geometry at different sections

desired geometry of the cross sections of two adjacent groves. Here b is the depth of the groove on the die surface and h is the pitch of the grooves. To investigate the effect of the groove geometry on the result of forming five distinct sets of the grooves were generated on the die surface. Correspondingly surface of the die was divided in five sections. The actual shape of the die differed from the designed geometry. This difference was due to slipping of cutting tool and vibrations of tool and workpiece in the course of turning. While the designed groves had a triangular profile, due to the limitations of the machining facility used for die manufacturing the grooves and ridges generated on the die surface had a shape of a trapezium. It should be noted that the accuracy of machining of the die surface changes across the die radius. The accuracy of the

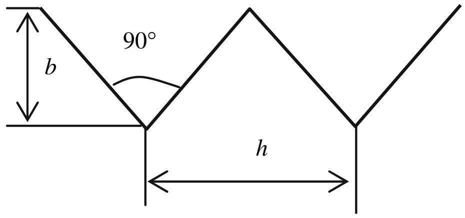

Fig. 13 Desired geometry of the ridges generated on the die surface

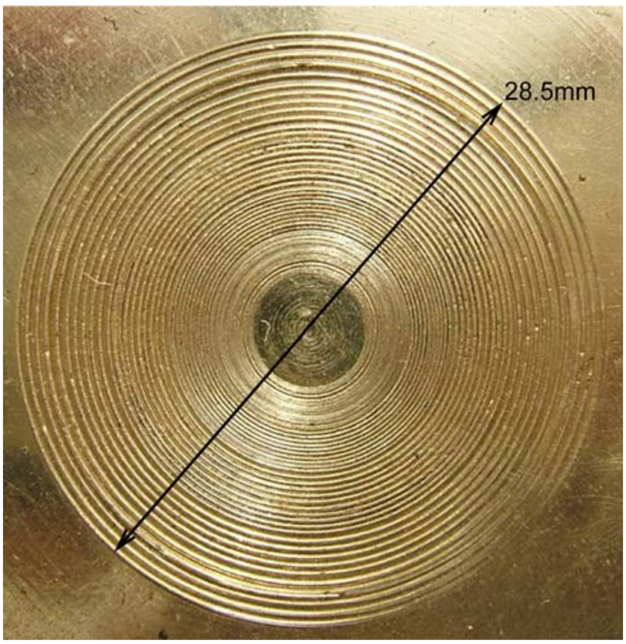

Fig. 14 General view of concentric grooves and ridges formed on the surface of a brass sample. Notice the compliance of the geometries of the die and the workpiece

Sections 3-5 was adequate while the larger deviations from desired geometry were found within the Sections 1 and 2. In this study, the compliance between the die geometry and the geometry of the generated surfaces was investigated.

A general view of the surface of a brass target generated in the course of forming is shown in Fig. 14. A similar geometry was formed on a copper plate as well (Ref 10). As it follows from Fig. 14, the microscale geometries of the die and the workpiece complied sufficiently well and the geometries of the grooves and ridges on both surfaces are almost identical. Full scale scanning of samples was performed using infinite focus microscopy. This accurate reproduction of the die geometry was observed in all sections.

To quantify the accuracy of forming the microscopic evaluation of a workpiece was carried out by two methods, infinite focus microscopy and 3D digital microscopy. The performed examination confirmed that at the existing tolerances of die fabrication, there is sufficient compliance between the desired die geometry and the actual geometry of a workpiece.

The surface geometry generated in the course of an impact of a brass sample is shown in Fig. 15 and 16. An infinite focus microscopy example of 3D image of lateral segment of concentric grooves and ridges formed on surface of brass is shown in Fig. 15 and one profile of the same segment is shown in Fig. 16. Detailed scanning of formed geometry confirmed compliance between the die and forged surfaces. Trapezium angles of ridges are mirror images of corresponding angles of grooves. This was confirmed by both inspections.

6.2 Fine Stamping

The objective of these experiments was study of the formation of complex patterns on a target surface. In this case a conventional coin was used as a supporting die. Target materials included copper, brass, aluminum, and high-ductility steel. The steel had 46% elongation, tensile strength of 325 MPa, and yield strength of 195 MPa. Thickness of the copper and brass samples was 3 mm and steel samples were 2.5 mm thick. As a result, the coin image was stamped into

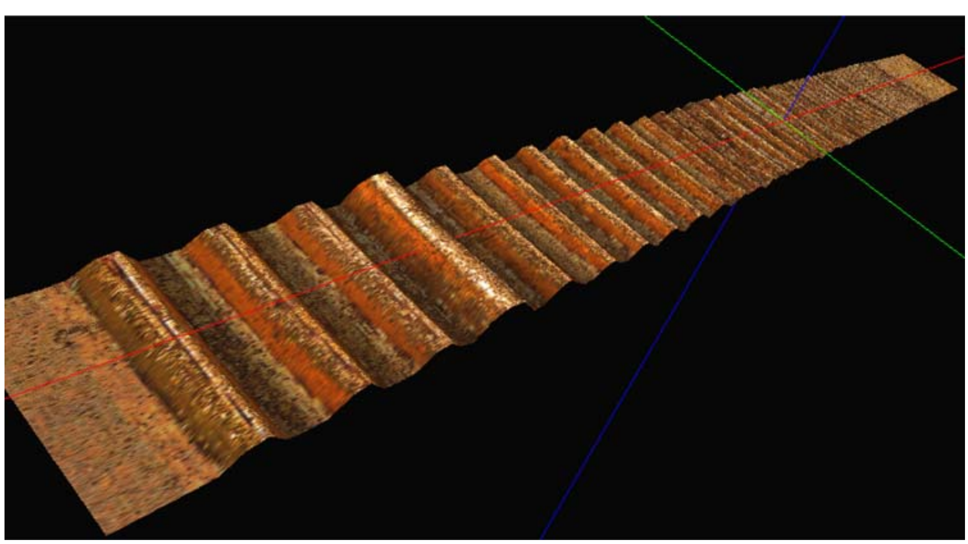

Fig. 15 3D image of a lateral segment of concentric grooves and ridges formed on the surface of the brass sample. Notice that ridges and grooves of the workpiece surface have the forms of a trapezium which is similar to a corresponding segment of the die

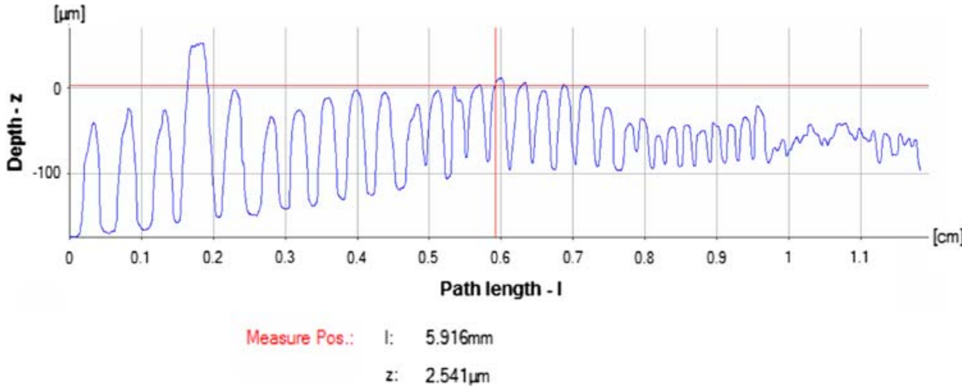

Fig. 16 Example of the profile of a lateral segment of the concentric grooves and ridges formed on the surface of a brass

Fig. 17 3D image of a coin formed on copper

copper, steel, and aluminum plates. A calculated impact velocity was 850 m/s. Geometry of the coin was accurately reproduced on all samples. Quality of reproduced surface was characterized by three methods: infinite focus microscopy and 3D profile analysis and scanning electron microscope. Measurement of parameters of the surface geometry was performed and it was demonstrated that the coin geometry was reproduced sufficiently accurate on the surface of all targets.

General view of a coin stamped on copper is shown in Fig. 17 and 18. Measurements of the original coin geometry revealed that it corresponds to the topography of the coin.

7. Experimental Investigation of Microforming

7.1 Microns Scale Forging

Previously (Ref 10, 15) it was demonstrated that liquid projectiles can be used to form microchannels on the surface of different metal parts. Individual microchannels (Fig. 19) and networks of the microchannel (Fig. 20) were formed on copper, brass, and steel samples. Tungsten wires 7 and 40 µm diameter

Fig. 18 General view of a coin stamped on copper and original coin used as a die. Notice reproduction of fine details of the coin on the sample surface

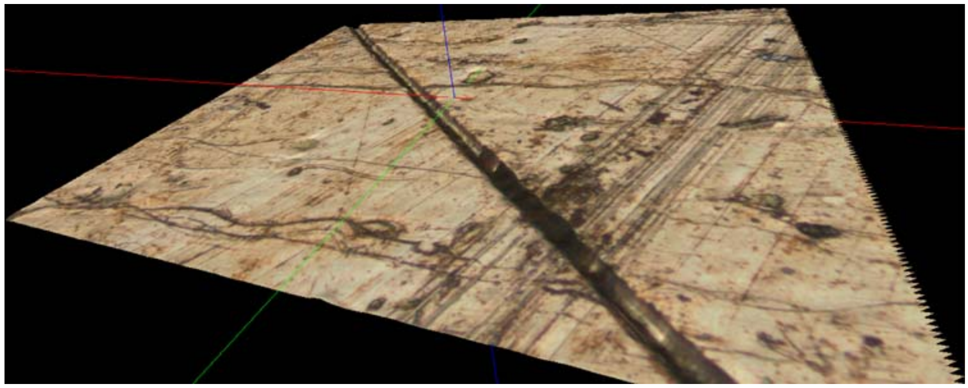

Fig. 19 3D image of a microchannel formed on a steel plate

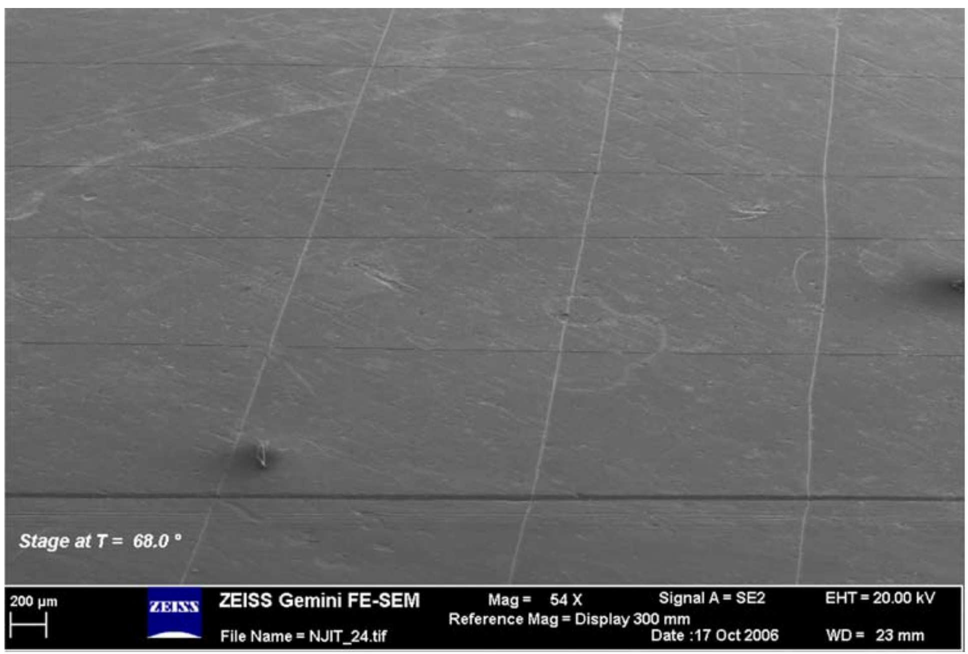

Fig. 20 SEM image of a microchannels network formed on the surface of a brass sample

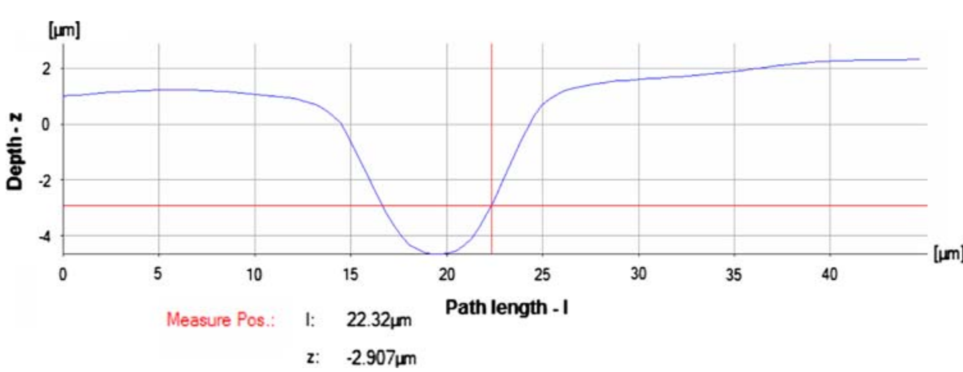

Fig. 21 The profile of a microchannel created on the steel sample shown in Fig. 19. The scales of the *X*- and *Y*-axes are given in microns

were used as dies. Microchannels were formed as water projectiles impacted working metal plates which drove tungsten wires into softer materials of samples creating a desired network of microchannels. As a result of detailed investigation of the surface topography feasibility of the use of water projectiles for microscale forming was confirmed.

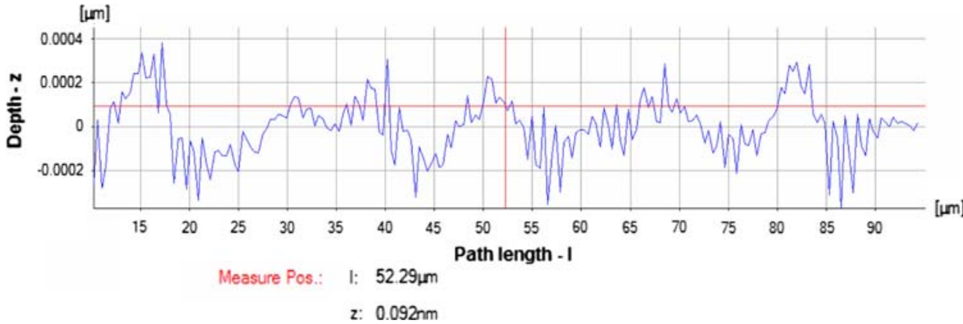

Fig. 22 Roughness of the virgin surface of the steel sample shown in Fig. 19. Scales of the *X*- and *Y*-axes are given in microns

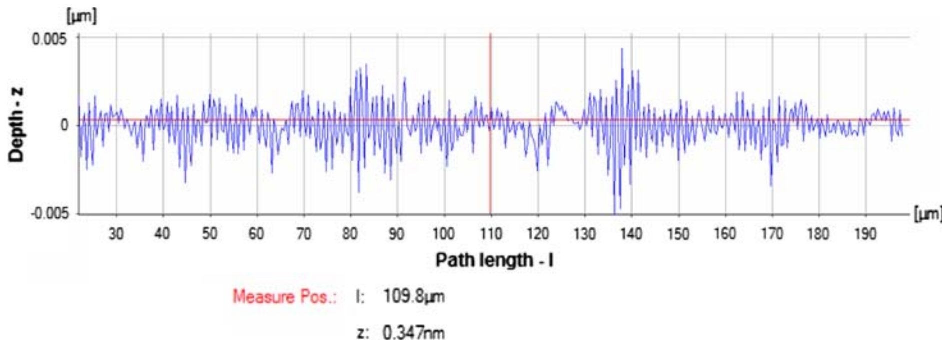

Fig. 23 Roughness of the bottom of a section of the microchannel shown in Fig. 19. Scales of the X- and Y-axes are given in microns

The objective of this study was to investigate the dimensional consistency of created microchannels and the effect of a liquid impact on mechanical properties of impacted metals. A 3D image of microchannel formed on brass by 7 µm diameter tungsten wire is shown in Fig. 19. The image was created using the infinite focus microscopy. This device enabled us to evaluate the profile, the waviness, and the roughness of the generated microgrooves. Profile measurements were performed in the dense manner to investigate dimensional consistency of the formed channels. A typical section of a microchannel depicted in Fig. 19 is shown in Fig. 21, which illustrate the compliance between the geometries of the die and the formed channel. The roughness of a steel plate (Fig. 19) prior to the impact was 0.0006 µm, while the roughness of the bottom of the generated microchannel was 0.005 µm (Fig. 22 and 23). The performed measurements show that the geometry of the generated microchannels was sufficiently stable.

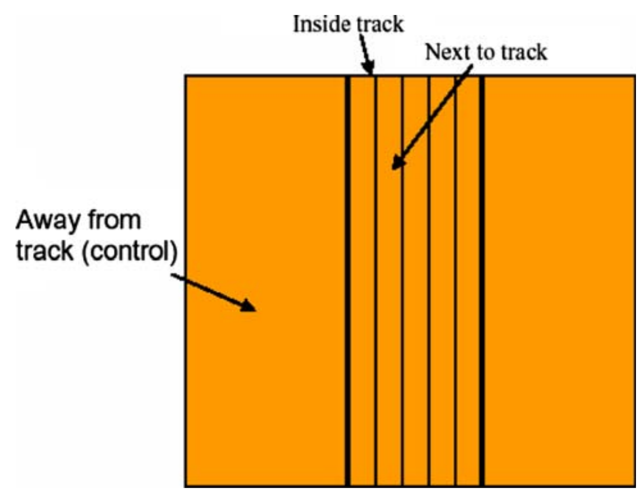

Fig. 24 Cartoon image of areas where samples properties were measured

7.2 Mechanical Properties of the Formed Surface

Mechanical properties of the microchannels including the hardness and the reduced modulus were measured by the use of a Tribo-Indenter. Properties of the brass, steel, and copper samples were investigated. In performed measurements a tested area was imaged by an optical microscope prior to testing to determine indent location and then Scanning Probe Microscope images with the same tip after testing. The areas inside a microchannel (inside track), next to a microchannel (next to the track), and away from a microchannel (away form the track) were tested (Fig. 24).

The Tribo-Indenter is a high-resolution nanomechanical instrument that performs nanoscale indents by applying a force to the indenter tip while measuring tip penetration into the sample body. During indentation, the applied load and the tip displacement are continually measured, creating a load-displacement curve for each indent. Nanoindentation tests were performed on brass, steel, and copper samples. All indents had the maximal peak load of 2000 µN, and in-contact mode while Berkovich tip was used. Every quantitative indent included a 3 s linear hold at the peak load to stabilize any creep in the sample. Steady load cycle was applied throughout a testing. An example of the load-unload curves for testing a steel sample is shown in Fig. 25. Three tested areas are shown in Fig. 26 and 27. Each of

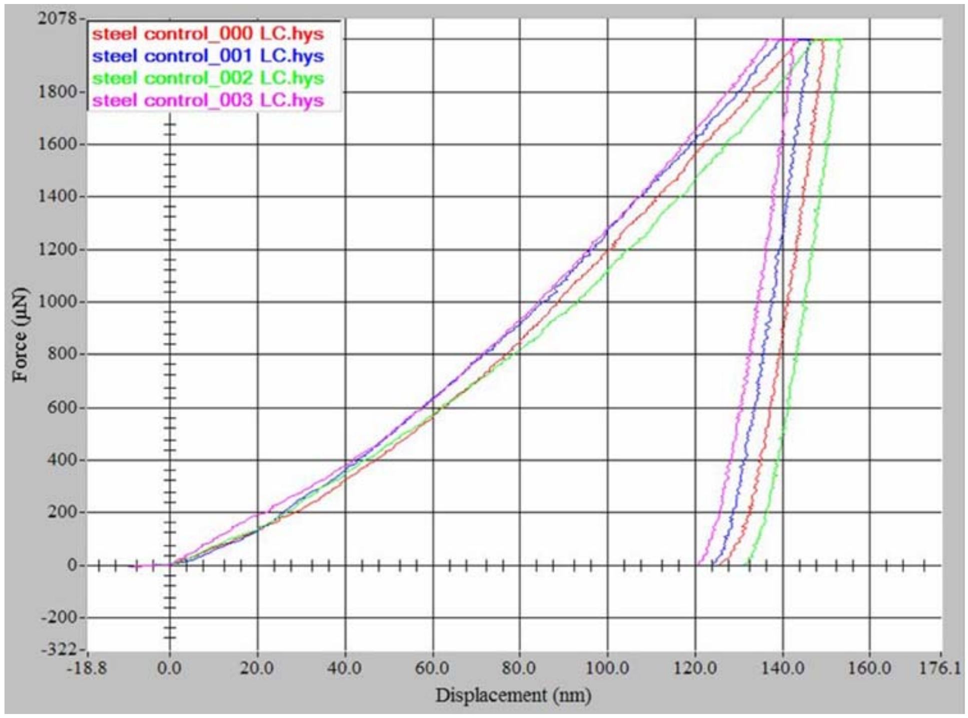

Fig. 25 Set of load-unload curves for testing of a steel sample

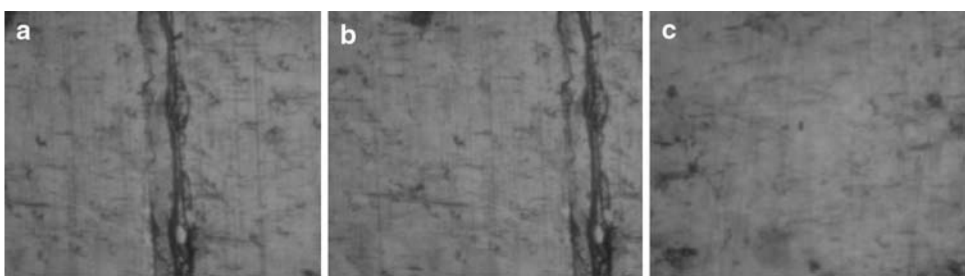

Fig. 26 Optical microscope images of areas tested on brass sample. (a) inside track, (b) next to track, and (c) control

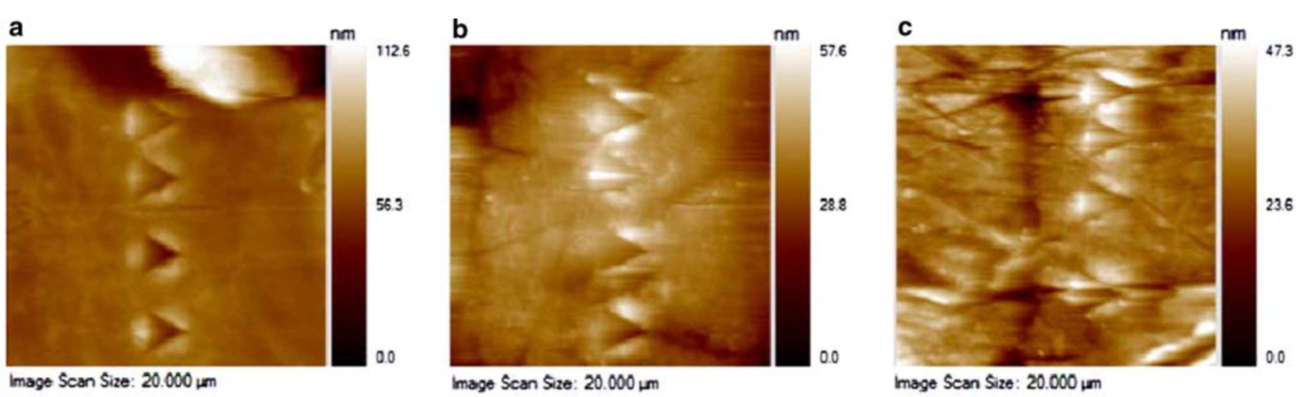

Fig. 27 SPM image after testing showing residual indent impressions left on sample surface. (a) inside track, (b) next to track, and (c) control

these areas had at least three indentations. Results of the measurements are summarized in Table 4 for a brass sample, in Table 5 for a steel sample, and in Table 6 for a copper sample.

The performed tests show the increase of the hardness and modulus inside a track comparatively to the top surface of the sample. The obtained Scanning Probe Microscope images demonstrate that this trend is not topography dependent. The

Table 4 Results of the nanoindentation testing of a brass sample

	Brass		
	In track	Next to track	Control
Hardness, GPa	3.39 ± 0.05	2.80 ± 0.28	2.94 ± 0.14
Modulus, GPa	116.44 ± 4.96	115.45 ± 2.72	117.69 ± 4.48

Table 5 Results of nanoindentation testing of steel sample

	Steel		
	In track	Next to track	Control
Hardness, GPa	4.32 ± 0.14	3.16 ± 0.24	3.40 ± 0.21
Modulus, GPa	168.4 ± 5.29	165.00 ± 6.52	149.31 ± 5.53

Table 6 Results of the nanoindentation testing of copper sample

	Copper		
	In track	Next to track	Control
Hardness, GPa	2.58 ± 0.26	2.11 ± 0.17	2.22 ± 0.45
Modulus, GPa	156.53 ± 14.50	134.53 ± 7.90	120.95 ± 15.14

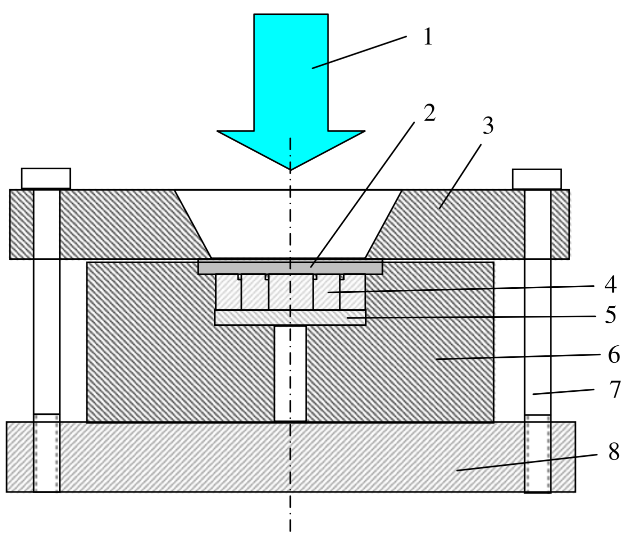

Fig. 28 Schematic of experimental set up for microextrusion 1—water projectile, 2—working sample, 3—fastening plate, 4—integrated rings die, 5—supporting plate, 6—die-holder, 7—, and 8—main support.

standard deviations of the obtained measurement results are low. This shows that the liquid impact generates a stable surface.

7.3 Micron Scale Extrusion

In the previous study, it was demonstrated that the liquid projectiles can be used for micron scale extrusion of metals

Fig. 29 Extruded circular brass rings

Fig. 30 Digital reproduction of extruded small brass ring (central ring on Fig. 29)

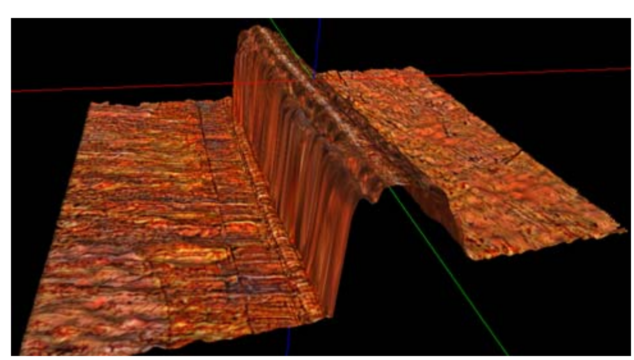

Fig. 31 3D image of a section of the extruded copper ring. The section is 450 μm high and 200 μm thick

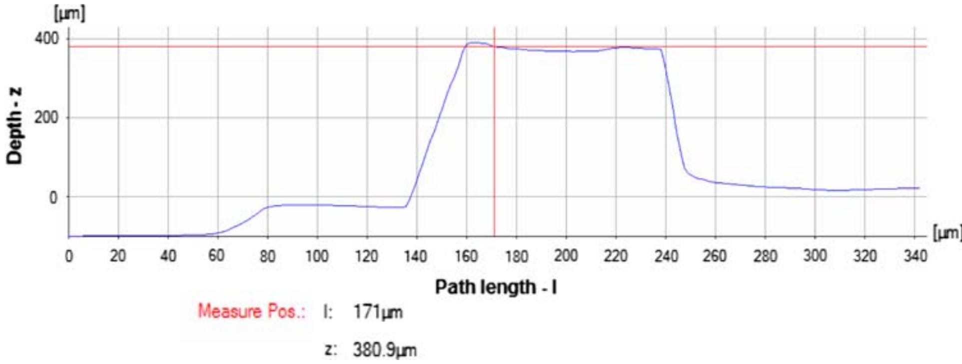

Fig. 32 Profile of a section of the extruded copper ring

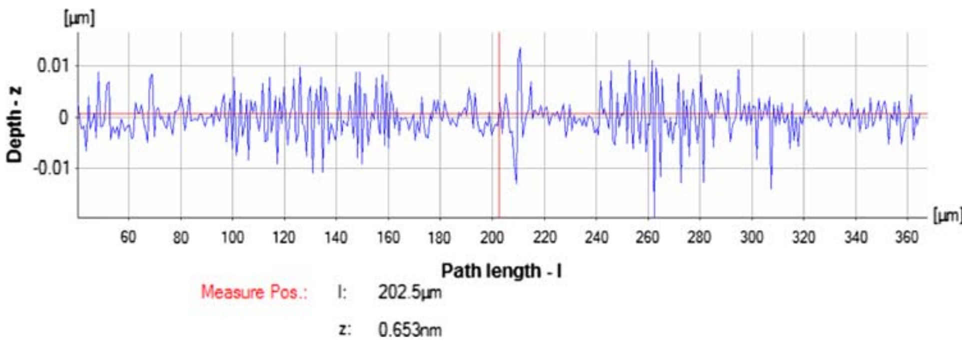

Fig. 33 Roughness of segment of the die surface

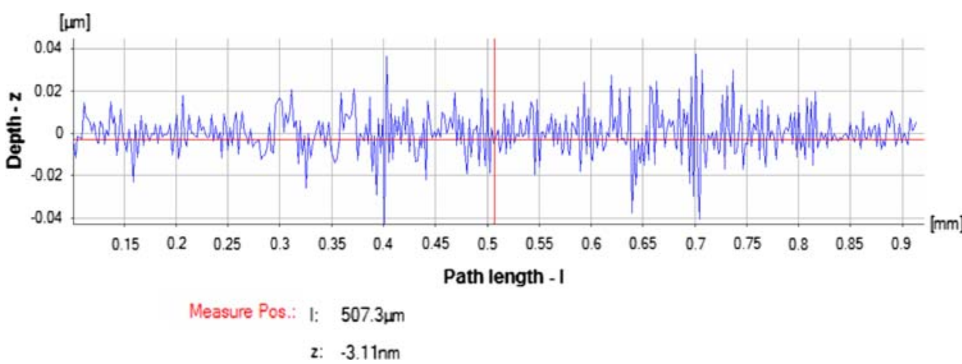

Fig. 34 Roughness of a section of the extruded copper ring

(Ref 10). Extrusion of metals by filling a space between cylindrical and plane walls was investigated using an experimental setup (Fig. 28). The distance between the walls ranged from 10 to 50 µm, while the wall length was in order of several centimeters and the height was in order of several millimeters. Thus, process involves filling a semi-infinite micron scale gaps by an impacted metal. Copper, brass, and high-ductility steel samples were used. The heights of the rings and the cylinder were almost precisely equal. While the thickness of the rings was in order of microns, the height and the diameter were in order of millimeters. Thus microextrusion with comparatively high-extrusion ratio was accomplished. A general view of the extruded rings is shown in Fig. 29 and a digital reproduction of a ring from Fig. 29 is shown in Fig. 30. This ring was extruded and completely separated from the parent brass plate. The internal diameter of the ring was 15 mm and a comparatively uniform ring thickness was 100 µm. In the previous study, extrusion ratio ranging between 10 and 130 was achieved.

An infinite focus microscopy was used for investigation of the compliance between the geometries of the generated thin film and the die. A 3D image (Fig. 31) and a profile (Fig. 32) of a section of the extruded copper ring with inclined wall were constructed and the inclination angles were measured and compared with that of the die opening. The compliance of the opening and the film geometry was demonstrated. The roughness of the die (Fig. 33) and that of the ring (Fig. 34) are also similar. It should be noted that the ring roughness does not exceed 1 µm. The performed experiments demonstrate feasibility to generate thin film using the liquid impact.

8. Discussion of Results

The performed experiments involved study of variety forming operations, such as punching, forging, coining at the macro-, and microscales. The facilities used (launchers, dies) as well as the samples were fabricated in-house. At these conditions practically all performed tests were successful and resulted in the formation of samples having a desired shapes and high-quality surfaces. While forming facilities was rather simple, advance examination techniques were used for evaluation of geometry, topography, and mechanical properties of the generated samples. The obtained results of the measurement show good compliance between the geometry of dies openings and the shapes of the generated parts. It was also found that the liquid impact improves topography of the generated parts and at the very least does not reduce surface quality.

9. Conclusions

It is shown that liquid impact-based forming has unique technological advantages. For example, similarly to the explosive forming, it requires a single die. The second die is replaced by a liquid punch. This simplifies the forming facilities and reduces its cost. Most of all this enables us to increase dramatically the process accuracy. Precision control of a launcher position and subsequent precision control of the projectile trajectory is a realistic and inexpensive task. Another significant process advantage is its versatility. A water projectile (liquid punch) could be applied to several different material processing operations. The rate of the tasks execution is determined by the firing rate of a launcher which realistically can be in order of Hz's. Thus a rapid process execution would enable mass production of various parts. Contactless mode of the launcher-workpiece interaction, ability of a liquid projectile to adjust to any geometry of a die, simplicity of process control assures the flexibility of the impact-based macro-, meso-, and microforming. The performed experiments demonstrated feasibility of the use of water impact for metal punching, forging, and stamping. However, the most promising process application is feasibility of mass production of microscale parts.

Acknowledgments

The support of NSF (Award DMI-9900247) and CRDF (UE2-2441-DO-02 Q2) in performing of this study is acknowledged. The state of the art instrumentation techniques was provided by EXCEL Technologies, Enfield, CT 06083; Hitachi High Technologies America, Inc, Gaithersburg, MD 20878; Micro Photonics Inc. Irvine, CA 92618; and Hysitron, Minnesota.

References

1. E.S. Geskin, B. Goldenberg, and G.A. Atanov, Investigation of Metal Piercing Using High-Speed Water Slugs, *Proceedings of 2001 WJTA American Waterjet Conference*, M. Hashish, Ed., Minneapolis, MN, USA, p 395–412
2. O.P. Petrenko, E.S. Geskin, B. Goldenberg, G.A. Atanov, and A.N. Semko. Investigation of the High Speed Water Slugs. *Proceedings of the 2003 Water Jet Technology Conference*, M. Hashish, Ed., Houston, TX, USA, Nov 2003, p 75–78
3. O. Petrenko, E.S. Geskin, G.A. Atanov, A.N. Semko, and B. Goldenberg, Investigation of Material Fracturing by the High Speed Water Slug, *Proceedings of 2003 DMII NSF Grantees Conference*, Birmingham, AL, Jan 2003, p 158–165
4. E.S. Geskin, V. Samardzic, O. Petrenko, T. Bitardse, G. Atanov, A. Semko, A. Kovaliov, and O. Rusanova. Feasibility Study of the Solid Freeform Fabrication of Heterogeneous Parts Using the Liquid Impact, *Proc. NSF DMII Grantees Conference 2005*, Scottsdale, Arizona, p 207–210
5. V. Samardzic, E.S. Geskin, G.A. Atanov, A.N. Semko, and A.V. Kovaliov, Investigation of Metal Processing Using A High Speed Liquid Impact, *Proceeding 2007 Conference of the Waterjet Technology Association*, Houston, Texas, Aug 2007, Paper 3B-3
6. M.D. Verson, *Impact Machining*, Verson-Allsteel Company, 1969
7. J.S. Reinhart, *Explosive Working of Metals*, Macmillan, 1963
8. A.V. Krutin et al. *Explosion Deformation of Metals*, Metallurgia, Moscow, 1975 (in Russian)
9. V. Samardzic, O. Petrenko, E.S. Geskin, G.A. Atanov, and A.N. Semco, Innovative Jet-based Material Processing Technology, *2005 WJTA American Waterjet Conference & Exhibition*, M. Hashish, Ed., Houston, TX, Aug 2005, Paper 2A-2
10. V. Samardzic, E.S. Geskin, GA. Atanov, A.N. Semko, and A.N. Kovaliov, Investigation of Liquid Based Material Micro-forming Technology, *J. Mater. Eng. Perform.*, 2007, **16/3**, p 375–389
11. Dohda, K., An overview of Micro-Forming Research and Development in Japan, *Micro/Meso Mechanical Manufacturing Workshop*, Gifu University, Yanagido, Gifu, Japan, 2000
12. H.-J. Lee, N.-K. Lee, S.-M. Lee, G.-A. Lee, and S.-S. Kim, Development of Micro Metal Forming Manufacturing System, *Mater. Sci. Forum*, 2006, **505–507**, p 19–24, Trans Tech Publications, Switzerland
13. Friedrich-Alexander University, Micro Forming Technology, http://www.lft.uni-erlangen.de/SEITEN/GRUPPEN/MUT/index_e.html
14. New Tool Technology by Direct Heating with Laser Radiation, *Mass Micro News Letter*, Sept 2006, (4), http://www.masmicro.net/Article/A243.pdf
15. V. Samardzic, E.S. Geskin, G.A. Atanov, A.N. Semko, and A.V. Kovaliov, Investigation of Metal Microforming Using High Speed Liquid Impact, *Proceeding 2007 Conference of the Waterjet Technology Association*, Houston, Texas, Aug 2007, Paper 1G